Final Report for AOARD Grant 104057 "**Graphene Nanowalls as Ingenious Material for Catalysts and Superconductors**"

March 12, 2011

Name of Principal Investigators: Dr. Kuei-Hsien Chen
- e-mail address : chenkh@pub.iams.sinica.edu.tw
- Institution : Institute of Atomic and Molecular Sciences, Academia Sinica
- Mailing Address : PO Box 23-166, Taipei, Taiwan
- Phone : +886-2-2366-8232
- Fax : +886-2-2362-0200

Period of Performance: 01/01/2010 – 12/31/2010

Abstract:

We've developed two approached for the growth of graphene, namely, thermal CVD for large area transferrable graphene and MPECVD for graphene nanowalls (GNWs). Defect density and carrier mobility studies using Raman microscopy and Hall measurement, respectively, have been carried out. A correlation between defect density and mobility has been reported. On the other hand, GNWs offers large surface area and excellent transport for applications in electrochemistry. It's found that residual strain of the GNWs is the key for enhanced catalytic activity when Pt nanoparticles were deposited. Detailed measurement and characterization using synchrotron radiation have been performed.

Introduction:

Graphene has attracted tremendous attention due to its unique properties and potential for optoelectronic applications. The awarding of 2010 Physics Nobel has further emphasized its importance. While many exciting properties of graphene has been reported, more discoveries are emerging in weekly basis. In respond to such fast growing field, we took two different experimental routes to explore the new field. One is to grow mm area graphene transferrable to other substrates, which allows subsequent patterning for electric and magnetic measurements. The other one is to grow graphene of ultrahigh surface area, which is important for electrochemical and energy applications.

In the past year, we've established the foundation for the proposed experiments. By thermal CVD on a copper substrate, up to 10 cm graphene can be synthesized and transferred to any designated substrate. While the quality of the film leave room to be improved, graphenes with mobility of 1200 cm^2/Vsec can be routinely produced. This opens up further studies on the defect doping and device fabrication utilizing such noble material. On the other hand, our microwave plasma enhanced CVD growth of graphene nanowalls (GNWs) produces sheet-like nanowalls standing up from a silicon substrate. The surface area of the graphene thus produced is orders of magnitudes higher than ordinary graphene, resulting in much reduced interface impedance. Various applications in electrochemistry will thus be possible utilizing GNWs.

Experiment:

Synthesis of transferrable graphene:

Graphene films, with different degree of disorder, were prepared by controlling the growth conditions in CVD processes. The CVD-graphene, grown on Cu foils, were then transferred by using a sacrificial poly(methyl methacrylate) (PMMA) layer as previously reported in literature. For comparison, MCG was also obtained by repeatedly pealing a small piece of highly ordered pyrolytic graphite (HOPG). Si wafer coated with 300 nm SiO_2 layer was used as substrates for all graphene samples. Figure 1 shows the process schematic of graphene growth where several parameters were tuned in order to study their influences on the graphene quality. These include the annealing and growth temperature (900 to 1000^{0}C), H_2 annealing time (15 to 60 min), H_2/CH_4 ratio (0 to 10) during growth, growth time (2 to 30 min), and the gas phase compositions during cooling stage (with or without H_2).

Raman and Hall measurements:

Report Documentation Page

Form Approved
OMB No. 0704-0188

1. REPORT DATE	2. REPORT TYPE	3. DATES COVERED
30 MAR 2011	**Final**	**25-02-2010 to 24-02-2011**

4. TITLE AND SUBTITLE	5a. CONTRACT NUMBER
Graphene Nanowalls as Ingenious Material for Catalysts and Superconductors	**FA23861014057**
	5b. GRANT NUMBER
	5c. PROGRAM ELEMENT NUMBER
6. AUTHOR(S) **Kuei-Hsien Chen**	5d. PROJECT NUMBER
	5e. TASK NUMBER
	5f. WORK UNIT NUMBER
7. PERFORMING ORGANIZATION NAME(S) AND ADDRESS(ES) **Academia Sinica,1 Roosevelt Rd., Section 4,Taipei 106,Taiwan,NA,NA**	8. PERFORMING ORGANIZATION REPORT NUMBER **N/A**
9. SPONSORING/MONITORING AGENCY NAME(S) AND ADDRESS(ES) **AOARD, UNIT 45002, APO, AP, 96338-5002**	10. SPONSOR/MONITOR'S ACRONYM(S) **AOARD**
	11. SPONSOR/MONITOR'S REPORT NUMBER(S) **AOARD-104057**

12. DISTRIBUTION/AVAILABILITY STATEMENT
Approved for public release; distribution unlimited

13. SUPPLEMENTARY NOTES

14. ABSTRACT
This is the report of a preliminary study to prepare and characterize graphene via chemical vapor deposition for large area transferrable graphene, and microwave plasma-enhanced chemical vapor deposition for graphene nanowalls.

15. SUBJECT TERMS
Catalysis, Graphene, Superconductivity

16. SECURITY CLASSIFICATION OF:			17. LIMITATION OF ABSTRACT	18. NUMBER OF PAGES	19a. NAME OF RESPONSIBLE PERSON
a. REPORT	b. ABSTRACT	c. THIS PAGE			
unclassified	**unclassified**	**unclassified**	**Same as Report (SAR)**	**7**	

Raman spectra of these graphene films on SiO_2/Si wafer were recorded by using Jobin-Yvon LabRAM H800 with He-Ne laser of 633 nm as excitation source. Spectra in several positions inside the continuous films were taken for checking the uniformity. Hall measurement was performed on the whole transferred graphene films by using ECOPIA Hall measurement system HMS-3000 with silver paint used as electrodes at the four corners of graphene films. The measurements were conducted in ambient surroundings with a constant current and magnetic field of 10 μA and 0.55 T, respectively, and the values of sheet resistance, carrier concentration, and carrier mobility were derived by using Van der Pauw method. The electrical field effect was investigated by using the same devices. Two of the silver paint electrodes across the whole films were used as source and drain electrodes. With 300 nm SiO_2 working as an insulator layer, back gate voltage was applied on Si. Figure 1(a-b) shows (a) a picture of transferred graphene films about 1 × 1 cm^2 on SiO_2/Si wafer and (b) the device schematic for electric field effect characterization.

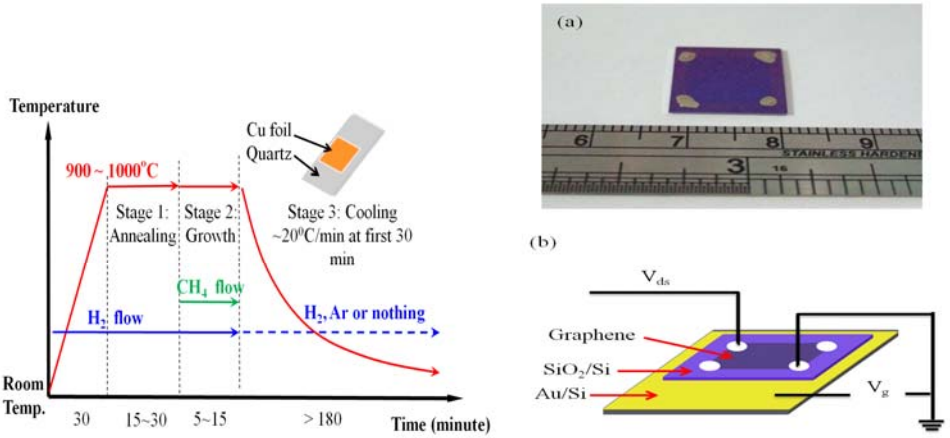

Figure 1: Illustration of the graphene growth process. Typically, the annealing and growth temperature was 950 ^{0}C. With a continuous H_2 flowing (10 sccm for the whole process), CH_4 with 50 sccm was introduced for 15 min during growth stage. On the right: (a) A picture of the transferred graphene on SiO_2/Si wafer with silver paint as electrodes at four corners; (b) device schematic for electric field effect charaterization.

Synthesis of graphene nanowalls:

Preparation of graphene-wraped SiC nanowalls was carried out in an AsTex 5kW microwave chamber. The growth of hybrid nanostructure was conducted in the following stages. Firstly, H_2 (99.999%) was introduced into the chamber to generate H_2 plasma to remove native oxide on Si surface at 800 ^{o}C at 40 Torr for few minutes, while the microwave power was fixed at 1500 W. Subsequently, a gas mixture of H_2, CH_4 and SiH_4 was feeding into the chamber at 1100 ^{o}C at a chamber pressure of few tens of Torr and a microwave power of 1500-2000 W for the growth of SiC nanowalls. The final stage of hybrid nanowall synthesis ends up with H_2 plasma etching on the surface of SiC nanowalls to form graphene layers for a few minutes. During nanowall growth, the substrate temperature was monitored by an optical pyrometer (CHINO IR-H) through a quartz window.

Results and Discussion:

Figure 2(a) shows a representative spectrum of our samples wherein three peaks can be observed and are of important connection to the graphehe quality: D (~1350 cm^{-1}), G (~1580 cm^{-1}), and 2D (~2650 cm^{-1}) peaks. The G peak corresponds to the E_{2g} phonon at the Brillouin zone center, whereas the D peak is caused by the breathing mode of sp^2 atoms and activated with the existence of some defects, which could be edges, functional groups, or structural disorders. The intensity ratio of D to G peak (I_D/I_G) has been conveniently used for estimating the degree of graphitization (or crystallite size of graphene). The 2D peak, relating to the second order of zone boundary phonons, which cannot be seen in first order Raman spectra in defect-free graphite, is, on the contrary, the most prominent feature in graphene. The electronic structure of graphene is uniquely captured in this 2D peak, which evolves with the number of layers. The full width half maximum (FWHM) of 2D peak and the

intensity ratios of 2D to G peak (I_{2D}/I_G) both were considered as indices of graphene layer number. A series of spectra are shown in Figure 2(b). With the change of growth conditions, D peaks with different intensity ratios to G peak can be obtained. Typically, I_{2D}/I_G remains >1.3 and the 2D peak exhibits a FWHM between 35 and 45 cm^{-1}. These characteristics indicate that monolayer-dominant graphene films with different degree of defect density were obtained.

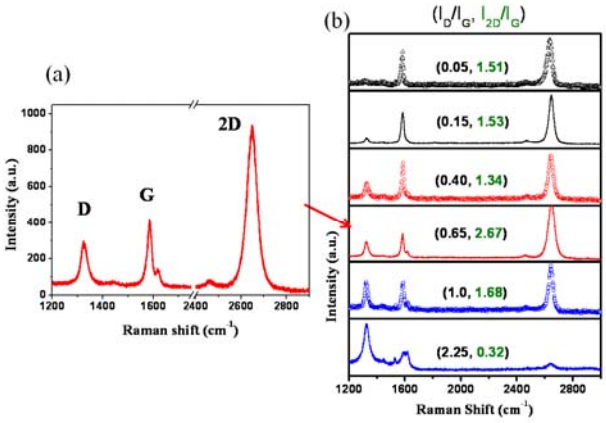

Figure 2: (a) Representative Raman spectrum of produced graphene films showing three important peaks of carbon materials: D, G and 2D peaks; (b) a series of Raman spectra of monolayer-dominant graphene films with different degree of defect density (I_D/I_G).

Figure 3 depicts the corresponding carrier mobility obtained by Hall measurements. All the data were collected from samples synthesized under different growth conditions but just classified according to two parameters: H_2/CH_4 ratio and the gas phase composition employed during cooling stage. It is clear that most graphene films prepared with H_2/CH_4 ratios ≤ 1 (typically we use 0.2) are showing carrier mobility > 500 $cm^2/V{\cdot}sec$ while the other groups have mobility much smaller than 500 $cm^2/V{\cdot}sec$. The carrier always shows *p*-type (except the sample with the lowest mobility) with sheet concentration ranging from 1 to 5×10^{12} cm^{-2}. A clear trend between mobility and defect density is then observed by using logarithmic fitting where black line is obtained using all data points with a correlation coefficient 0.81, and red line is based on samples showing I_{2D}/I_G >1.3 (monolayer dominant) with a correlation coefficient as high as 0.92. In summary, the crystallite size of graphene is estimated according to Raman spectra and the lower I_D/I_G ratio suggests less defect density in certain area. Therefore the scattering effect is suppressed and higher carrier mobility can be obtained. A logarithmic relation between carrier mobility and defect density is observed in our CVD-grown graphene films.

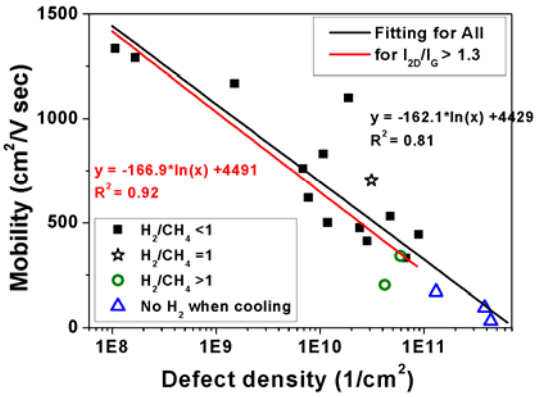

Figure 3: The carrier mobility of graphene samples corresponding to their calculated defect density, defined as $(1/L_a)^2$. The black square, black hollow star and green hollow circle represent H_2/CH_4 ratio less, equal and larger than 1, respectively; blue hollow triangle specifies samples prepared without H_2

incorporation at cooling stage. Black line shows a logarithmic fitting of all data points and red line is a fitting result based on those samples showing I_{2D}/I_G >1.3 (monolayer dominant).

The present approach produced uniform blackish deposition covering the entire Si substrate over a large area of 3.5x3.5 cm^2 as shown in Figure 4a. Typical field-emission scanning-electron-microscopy images of the as-grown product are shown in Figures 4 b-c. Edge-oriented wall-like nanostructures with ultrathin thickness (4-10 nm) can be clearly identified and the as-grown GNW have a typical length of 1-2 μm (Figure 4f).

Typical X-ray diffraction (XRD) pattern of the as-grown GNW is shown in Figure 1d with clear signature of 2H-SiC (100), (002) and (101) peaks. All reflections can be well-indexed to hexagonal 2H-SiC with lattice constants of a = 3.073 Å and c = 5.042 Å, in good agreement with the literature values of a =3.076 Å and c = 5.048 Å. Figure 1e shows the representative Raman spectrum of GNW, which is an effective tool to determine the polytypes of SiC. The sharp peak, with a full-width-at-half-maximum (FWHM)~ 6 cm^{-1}, at 756 cm^{-1} along with a broad band at 793 cm^{-1} can be assigned to the transverse optical (TO) phonon modes while the peak at 957 cm^{-1} can be ascribed to longitudinal optical (LO) phonon mode of SiC. The peak observed in the low-frequency regime (264 cm^{-1}), as shown in the inset of Figure 4e, corresponds to the transverse acoustic (TA) mode. All these Raman modes confirm the phase to be 2H-SiC polytype, which is consistent with XRD results. It is worth mentioning that the occurrence of a broad band (~856-860 cm^{-1}) between TO and LO modes may be related to the interface-like mode which has been reported in low-dimensional SiC nanostructures.

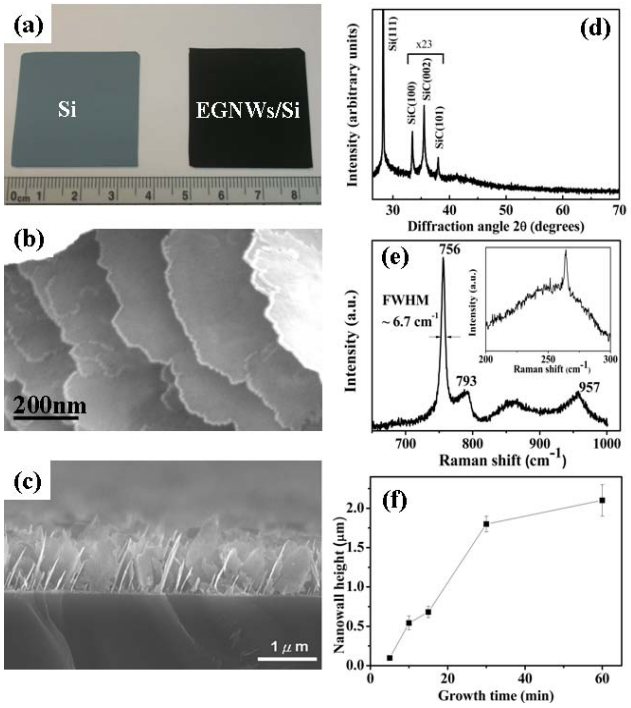

Figure 4. Morphology and structure of few-layer epitaxial graphene nanowalls (GNW) grown on Si(111) by MWPECVD. (a) Optical image of Si(111) substrate (left) and the substrate deposited with GNW (right). (b) Top view and (c) cross-sectional view FESEM images of GNW. (d) XRD pattern of SiC-templated graphene nanowalls. (e) Raman spectrum of GNW showing typical TO, LO and TA (inset) phonon modes of 2H-SiC. (f) GNW height as a function of growth time.

High resolution transmission electron microscopy (HRTEM) analyses of the GNW, shown in Figs. 5a-c, revealed a hybrid architecture composed of SiC nanowall scaffold sheathed by 1-4 layers of graphene. More interestingly, as shown in the selected area diffraction pattern in Fig. 5d, a predominant graphene orientation is rotated by 30° with respect to the underlying SiC scaffold, similar to the epitaxial graphene grown under ultrahigh vacuum (UHV) condition.

Figure 5e shows typical Raman spectra of the GNW with an average layer number of 3. For few-layer GNW, three prominent peaks were observed at 1363, 1602, and 2725 cm^{-1} which can be attributed to D band, G band, and 2D band, respectively. It should be emphasized that all Raman peaks in our few-layer GNW show significant blue-shifts as compared to HOPG and micromechanically cleaved graphene (MCG) obtained from HOPG of comparable layer thickness. This can be compared to EG grown atop SiC, in which significant blue-shifts were also observed and speculated to be attributed to the compressive strain induced by SiC substrate. Thus it is possible that the observed Raman blueshifts in our few-layer GNW could be caused by such SiC substrate-induced compressive strain. A close examination of the G and 2D peak positions with increasing layer thickness (n > 15) further supports the possibility of compressive strain by SiC. As evidenced in Figure 5f, GNWs with thicker layer (n >15) show a considerable red-shift for G (1584 cm^{-1} compared to 1604 cm^{-1}) and 2D (2705 cm^{-1} compared to 2725 cm^{-1}) peaks as compared to few layer GNW since the compressive strain can be relaxed as the layer thickness increases, which is in good agreement with the reported results obtained from UHV-grown EG. A pronounced defect-induced D band at 1364 cm^{-1} (Fig. 5e) suggests that few layer GNW contains defects, which can be attributed to factors such as edge effect due to its smaller size than that of the laser beam spot, strong interaction at graphene/SiC interface, vacancies and grain boundaries.

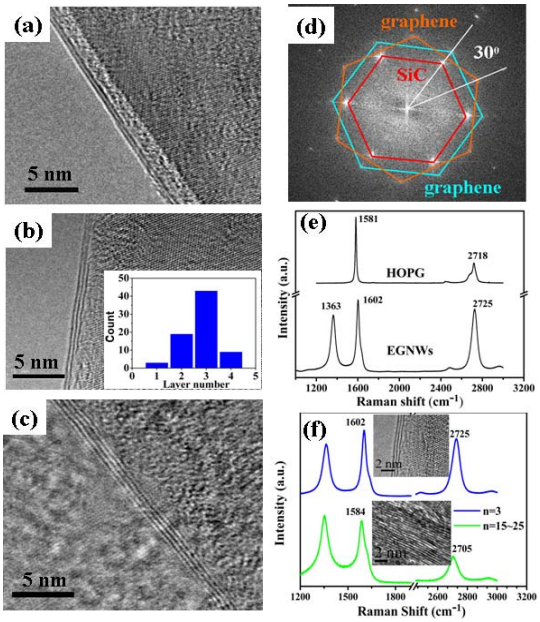

Figure 5. Microstructure characterization of GNW by TEM. (a)-(c) HRTEM images showing the edge region of GNW consisting of two (a), three (b) and four (c) graphene layers. (d) Electron diffraction pattern of few-layer GNW showing a predominant orientation of 30^0 with respect to the SiC spots. (e) Typical Raman spectra of few-layer GNW (n~3) and HOPG measured at 532 nm excitation line. (f) Detailed comparison of the G and 2D peaks of the few-layer GNW (n~3) and that of multi-layer GNW (n=15~25).

To investigate the chemical sensitivity of GNW, we fabricated solution gated field effect transistor (FET) on GNW and evaluated its pH response. The key features of the pH response of GNW-FET are presented in Figures 6a-d. Keeping a constant drain-source voltage (V_{DS}) of 0.3 V, all GNW-FETs were found to be predominantly p-type under all pH conditions (Figure 6b). A plot of drain-source current versus drain-source voltage (I_{DS}/V_{DS}) at a constant gate-source voltage (V_{GS}) of -0.5 V with increasing pH (Figure 6c) shows an obvious trend whereby at a constant V_{DS} of 0.3 V, conductance scales favorably in a linear fashion with increasing pH from pH 2 to 12 (Figure 6d). An increase in conductance with pH indicates the presence of an increasing negative potential gating effect caused by adsorbed hydroxide ions which induced an increase in hole density in GNW.

To gain insights into the ion dynamics at the graphene/electrolyte interface in different pH solutions, we performed frequency dependent impedance spectroscopy. Figure 6e shows the potential-capacitance plots in different pH solutions in which the anodic and cathodic capacitance

peak which centers around +0.2 V and -0.5 V corresponds to the electrochemical O_2/OH^- and $H_2/H3O^+$ redox couple respectively. The pH dependence of these capacitance peaks is clearly evident with a near Nernstian shift of 50 mV/pH units. Comparison with EG reveals thirty times increase in peak capacitance. This can possibly be related to the unique physical structures of GNW which offers a relatively large surface area to volume ratio for preferential adsorption of ions. The frequency dispersion of capacitance peaks performed in the potential range of -0.6 V to 0.6 V with frequencies ranging from 5 to 120 Hz suggests a slow ion adsorption/desorption behavior (Figure 6f). A careful examination of Figure 6f reveals a much sharper O_2/OH^- capacitance peak at pH 7 which suggests a preferential adsorption of hydroxide ions in an orderly manner on the GNW surface. These results emphasize that the increase in I_{DS} with pH can be adequately correlated to an increase in hole density induced by preferential adsorption of hydroxide ions on GNW. This underlines the potential of using GNW as chemical sensors.

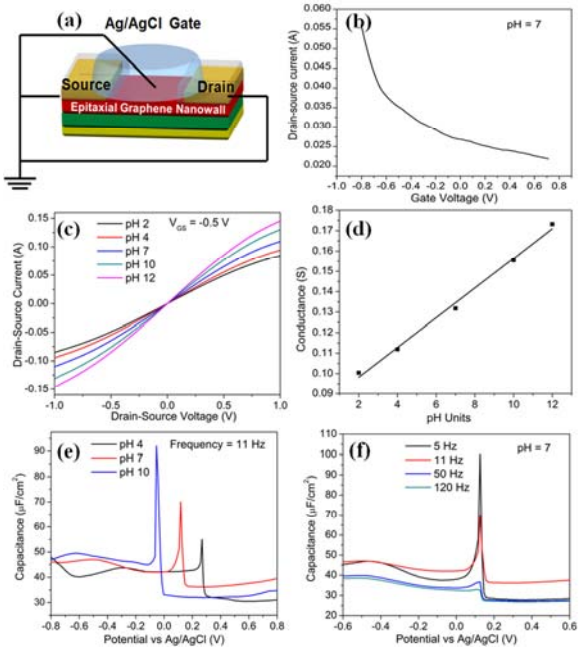

Figure 6. pH dependence of transfer characteristics and interfacial capacitance plots of GNW FETs. (a) Schematic representation of solution-gated FET device. (b) Transfer characteristics at pH 7 showing predominant p-type behavior at V_{DS} = 0.3 V. (c) Drain-source current as a function of drain-source voltage for pH values from 2 to 12 at V_{GS} = -0.5 V. (d) Conductance as a function of pH at V_{DS} = 0.3 V and V_{GS} = -0.5 V shows a linear relationship. (e) pH dependence of capacitance peak for redox couple O_2/OH^- and H_2/H_3O^+ at around 0.2 V and -0.5 V respectively. Frequency was kept constant at 11 Hz. (f) Frequency dispersion for adsorbed OH^- and H_3O^+ on GNW at around 0.2 V and -0.5 V respectively in 10 mM KCl/10 mM PBS at pH 7.

In summary, we have successfully prepared cm-scaled graphene films by using CVD process. Several parameters were studied for their effects on graphene properties. Raman spectroscopy was utilized to estimate the defect density by using D to G peak intensity ratios. The carrier mobility was obtained by Hall measurements and showed a clear correspondence with the defect density in graphene. With a typical process, graphene with carrier mobility ~1350 $cm^2/V{\cdot}sec$ and a calculated crystallite size ≥950 nm was obtained. Also, the neutrality point obtained from electrical field effect characterization progressively shifts to more negative gate voltage as defect density increases. The relationship between carrier mobility and defect density and the neutrality point shift due to defects are both observed for the first time in CVD-grown, large-scaled graphene. The characterization of defects is not fully explored, and further studies are underway to realize the kinetic mechanism, oxygen functionalization and the structural disorder in CVD-graphene.

Meanwhile, we have reported a large-scale growth methodology for few-layer strained GNW on Si substrate by MWPECVD and demonstrated its advantages in pH sensor. When applied as an

electrochemical electrode, the GNW exhibits nearly reversible redox characteristics, whereas as employed in the solution gated field effect transistor, the GNW shows a near-Nernstian behavior (50mV/pH) and a linear conductance-pH relation over a broad range of pH values (2-12). Further effort on the improvement for the strain control of few-layer GNW and detailed insight into the electronic properties for metal-support interaction could lead to better understanding on the strain induced catalytic enhancement. It is believed that the strained GNW with large surface area, controllable graphene layer number, and enhanced edges may hold great promise for use in catalysis, electrochemistry, biosensors, and energy conversion and storage devices.

List of Publications:

1. "*Correlating defect density with carrier mobility in large-scaled graphene films: Raman spectral signatures for estimation of defect density,"* J.Y. Hwang, C.C. Kuo, L. C. Chen, K. H. Chen, *Nanotechnology* **21**, 465705 (2010).
2. "*Few-layer strained graphene sheathed SiC nanowalls for heterogeneous catalysis and sensing application,"* M.S. Hu, C.C. Kuo, C.T. Wu, C.W. Chen, P. K. Ang, K.P. Loh, K.H. Chen and L.C. Chen, *Carbon* (communicated, 2011).
3. "*Raman spectroscopy of graphene prepared by CVD method: the disorder and temperature effects,"* J.Y. Hwang, C.K. Chang, C.C. Kuo, C.I. Huang, K.H. Chen, and L. C. Chen *Appl. Phys. Lett.* (communicated, 2011).

DD882: As a separate document, please complete and sign the inventions disclosure form.

This document may be as long or as short as needed to give a fair account of the work performed during the period of performance. There will be variations depending on the scope of the work. As such, there are no length or formatting constraints for the final report. Include as many charts and figures as required to explain the work. A final report submission very similar to a full length journal article will be sufficient in most cases.